

Photocurable Amphiphilic Perfluoropolyether/Poly(ethylene glycol) Networks for Fouling-Release Coatings

Yapei Wang,[†] Douglas E. Betts,[†] John A. Finlay,[§] Lenora Brewer,[⊥] Maureen E. Callow,[§] James A. Callow,[§] Dean E. Wendt,[⊥] and Joseph M. DeSimone^{*,†,‡}

[†]Department of Chemistry, University of North Carolina at Chapel Hill, Chapel Hill, North Carolina 27599, United States, [‡]Department of Chemical & Biomolecular Engineering, North Carolina State University, Raleigh, North Carolina 27695, United States, [§]The University of Birmingham, Birmingham, B15 2TT, U.K., and [⊥]Cal Poly, San Luis Obispo, Biological Sciences Department, San Luis Obispo, California 93407, United States

Received November 10, 2010; Revised Manuscript Received January 12, 2011

ABSTRACT: We demonstrate a facile way of cross-linking hydrophobic perfluoropolyethers, PFPEs, with a series of hydrophilic poly(ethylene glycol)s, PEGs, to prepare a range of amphiphilic networks for use as fouling-release coatings. The PFPE matrix of the networks endows the coating with a low surface energy while the PEG is added to weaken fouling adhesion. It is therefore envisioned that the coating surfaces of these optically transparent and mechanically robust films will display hydrophobicity leading to nonfouling and fouling release characteristics. Two kinds of functionalized PEG oligomers have been cross-linked with reactive, dimethacryloxy-functionalized PFPE oligomers to form a range of amphiphilic networks: (i) a monomethacryloxy-functionalized PEG macromonomer (454 g/mol) (PEG454-MA) which was used to yield blends with flexible PEG chains on the surface as well as in bulk and (ii) a dimethacryloxy-functionalized PEG (550 g/mol) (PEG550-DMA) which results in PEG chains that are relatively more restricted in the network blends and serve as an added difunctional cross-linker for the network along with the dimethacryloxy-functionalized PFPE. The PFPE/PEG cross-linked networks coated on a substrate show very low swelling characteristics in water when PEG454-MA comprises not more than 10 wt % of the overall composition or when PEG550-DMA is used and does not comprise more than 30 wt % of the overall composition. The PFPE/PEG454-MA coatings having PEG chains with one untethered chain end were found to display relatively high spore and barnacle release performance in comparison to PFPE/PEG550-DMA coatings which have the PEG chains in a more restricted network topology.

Introduction

The conventional approach to biofouling prevention in marine craft applications has been to use antifouling paints and coatings, which function through the release of toxins or other biocides in the immediate vicinity of a ship's hull through an ablative or leaching process.^{1–3} The use of such technology, while admittedly effective, has proven to be responsible for increases in the levels of organotin and other toxic compounds in or around dry docks, harbors and shipping lanes.^{4,5} Therefore, the development of minimally adhesive, mechanically durable, easy to apply, non-toxic, fouling-release coatings as responsible and practical alternatives to the currently used antifouling technologies is being urgently pursued.^{6–12} On one hand, it is suggested that surface energy and mechanical properties are the key factors to determine how the coatings can resist fouling attachment.^{13,14} In this regard, elastomers with a low surface energy and a low Young's modulus such as silicones^{1,15–21} and fluorinated polymers²² have been evaluated as good candidates to facilitate fouling release. In an effort to increase the fouling-release efficiency of these materials, antifouling polymers as well as biocidal substances have been blended into them.^{23–27} However, the inclusion of biocidal units increases the toxicity of the marine coatings which limits their wide application.²⁸ Rather than the inclusion of biocidal components, the combination of environmentally benign materials in

these elastomers is certainly regarded as a better choice. Poly(ethylene glycol), PEG, is well-known to inhibit protein as well as cell adsorption due to electrostatic repulsion and a hydration effect at the interface.^{29–33} Self-assembled monolayers of PEG or cross-linked PEG hydrogel coatings have been reported to exhibit good protein resistance.^{34–36} However, since hydrophilic PEG swells in water, these PEG-based coatings are not very effective for use as marine coatings because they lack durability. A new concept to blend PEG with low surface energy fluoropolymers to maintain the nonfouling property of the coatings as well as increase the coating stability has been exploited by the research groups of Wooley,^{37–39} Ober,^{40–42} and Galli.⁴³ To adequately blend PEG into a fluorinated matrix without serious phase separation resulting, Wooley et al. demonstrated a stepwise condensation polymerization to synthesize a hyperbranched fluoropolymer–poly(ethylene glycol) network for fouling release coatings.^{37–39} The evaluation of settlement and release assays of sporelings of the green alga *Ulva*, indicate this hyperbranched network exhibited good fouling-release performance. The Ober and Galli groups separately reported side-chain block copolymer consisting of grafted ethoxylated fluoroalkyl segments that can release both sporelings of *Ulva* and diatoms.^{40–43}

Previously we have reported the use of PFPE polymers as a unique class of high performance coating materials that have extremely low surface tensions (8–18 mN/m), a tunable modulus, and excellent thermal and chemical stabilities.^{44,45} Building upon these materials we have also established the utility

*Corresponding author. E-mail: desimone@unc.edu.

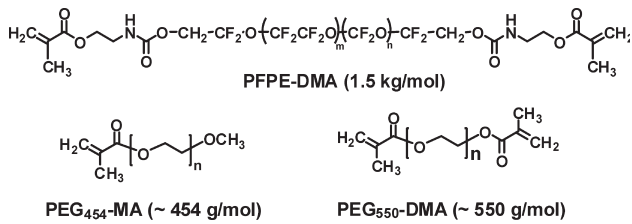


Figure 1. Molecular structures of the building blocks for PFPE/PEG blends.

of methacryloxy-functionalized PFPE materials copolymerized with methacryloxy-functionalized PEG segments using photoirradiation to generate a new family of amphiphilic networks.⁴⁶ Herein we report the use of this family of amphiphilic PFPE/PEG blends as nontoxic UV-curable, fouling-release coatings (Figure 1). Two kinds of PEGs were utilized for incorporation into amphiphilic networks with PFPEs: flexible monofunctional PEG and a restricted difunctional PEG. The antifouling/fouling release performance of the coatings was assessed by laboratory assays with barnacles and the green alga *Ulva*.

Experimental Section

Materials. 1,1,1,3,3-Pentafluorobutane (Solkane) was purchased from Micro-Care. The 1.5 kg/mol PFPE-diol (Fluorolink D10-H) was purchased from Solvay Solexis. Tetrabutyltin diacetate (DBTDA), α -hydroxycyclohexyl phenylketone (HCPK), 2-isocyanatoethyl methacrylate (IEM), poly(ethylene glycol) monomethacrylate (PEG454-MA, 454 g/mol), poly(ethylene glycol) dimethacrylate (PEG550-DMA, 550 g/mol), 3-aminopropyl trimethoxysilane, acryloyl chloride, triethylamine, and all solvents were purchased from Sigma-Aldrich. Standard glass (1 mm \times 35 mm \times 75 mm) was purchased from Fisher.

Synthesis of PFPE-DMA. Perfluoropolyether-dimethacryloxy-functionalized PFPE (PFPE-DMA) was synthesized according to our previous work.^{46,47} Briefly, PFPE diol (1.5 kg/mol) was first dissolved in 1,1,1,3,3-pentafluorobutane and reacted with a 2.05:1 molar ratio of IEM at 45 °C for 24 h, using 0.1 wt % DBTDA as a catalyst. The solution was then passed through a chromatographic column filled with alumina. After the solvent was evaporated, the product was filtered through a 0.2 μ m poly(ether sulfone) filter to yield a clear, colorless, viscous oil.

Synthesis of N-(3-(trimethoxysilyl)propyl)acrylamide (TSPA). The synthesis was conducted as previously reported in the literature.¹² Into 50 mL of tetrahydrofuran (THF) were dissolved 3-aminopropyl trimethoxysilane (2.74 g, 15.3 mmol) and triethylamine (2.32 g, 22.9 mmol). The mixture was cooled to 0 °C in an ice–water bath and then a solution of acryloyl chloride (1.50 mL, 18.3 mmol) in 20 mL THF was added dropwise. After stirring at 0 °C for 3 h, the suspension was filtered and then the solvent was removed under vacuum to yield a brown oil. The product was then washed with cold water and extracted with chloroform. The organic layer was dried over anhydrous Na₂SO₄ followed by evaporation of the solvent to afford the product. ¹H NMR (CDCl₃, 400 MHz, ppm): δ 6.26 (1H, d, *J* = 17.2 Hz, CH₂), 6.06–6.13 (1H, m, CH), 5.61 (1H, d, *J* = 10.0 Hz, CH₂), 3.55 (9H, s, OCH₃), 3.31–3.36 (2H, m, CH₂), 1.66–1.62 (2H, m, CH₂), 0.68 (2H, t, *J* = 8 Hz, CH₂).

Preparation of Glass Substrates. Fisher brand standard glass slides (1 mm \times 35 mm \times 75 mm) were boiled in piranha solution (H₂SO₄:H₂O₂ = 7:3) at 90 °C for 30 min, and then washed with deionized water. After being fully dried in an oven at 110 °C overnight, the glass sides were soaked in a *N*-(3-(trimethoxysilyl)propyl)acrylamide, TSPA, ethanol solution (1/100, v/v) for 12 h. Nonreacted excess TSPA on the glass surface was washed away with ethanol and then the residual solvent on the slides was

removed under vacuum at room temperature for 12 h. The successful functionalization of the TSPA on the glass slides was confirmed by X-ray photoelectron spectroscopy.

Preparation of Cross-Linked PFPE/PEG Blends. PEG454-MA and PEG550-DMA were first passed through an alumina chromatographic column (1 cm \times 3 cm) to remove the inhibitor. The PEG454-MA was then added to the desired amount of the PFPE-DMA precursor in a range of composition weight ratios of 5/95, 10/90, 15/85, 20/80, 25/75, 30/70, 50/50, and 70/30 to form a transparent homogeneous mixture. To the blend was then added 0.2 wt % of the photo initiator HCPK which was dissolved by vortexing. Since PEG550-DMA is not well miscible with PFPE-DMA, Solkane (1/10, v/w) was employed as the cosolvent to enhance the miscibility of PEG550-DMA with the PFPE-DMA. After vortexing for 5 min, colorless and clear, homogeneous liquid blends of PFPE-DMA and PEG550-DMA with composition weight ratios of 5/95, 10/90, 30/70, 50/50, and 70/30 were obtained. In the same way, 0.2 wt % HCPK photo initiator was dissolved in the mixture of PEG550-DMA and PFPE-DMA. The cross-linked PFPE/PEG films for mechanical, UV-vis spectroscopy, and environmental scanning electron microscope (ESEM) analysis were made of liquid PFPE/PEG blends fully cured in a PDMS mold (1 mm \times 35 mm \times 75 mm) by UV irradiation (Electronlite UV curing chamber model no. 81432-ELC-500, λ = 365 nm, irradiated for 10 min under N₂ purge). To covalently attach the PFPE/PEG films onto the glass substrate, the PFPE/PEG blends were cast onto TSPA-modified glasses (1 mm \times 35 mm \times 75 mm) and were exposed to UV irradiation for 10 min under N₂ purge. Finally, the films composed of PFPE/PEG550-DMA were kept under vacuum for 24 h to remove any residual Solkane solvent.

Ultraviolet–Visible Spectroscopy. UV-vis transparency measurements were performed on a Shimadzu UV-3600 UV-vis spectrophotometer over the wavelength range of 300–700 nm. Thin films of ca. 1 mm were measured for optical transparency with the percent transmittance at 550 nm.

Dynamic Mechanical Thermal Analysis. DMTA measurements were performed using a 210 Seiko Dynamic mechanical spectrometer, operating at a fixed frequency of 1 Hz in tension mode. The temperature was varied from –150 to +150 °C with a heating rate of 2 °C/min.

Atomic Force Microscopy. The surface topography of the coating films was imaged using an Asylum Research MFP3D AFM in tapping mode with silicon cantilevers from Mikromasch USA with a resonance frequency of 160 kHz, spring constant of 5.0 N/m, and radii of less than 10 nm.

Mechanical Properties. Stress-strain measurements were performed at ambient temperature on an Instron model 5566 system using a 10 kN load cell at a crosshead speed of 10 mm/min. An extensometer of 3 mm gauge length was used to measure the strain accurately. Young's modulus was determined from the stress-strain curves. Four replicates were performed for each sample.

Water Swelling. The free-standing cured PFPE/PEG films and those coated on glass were soaked in deionized water for 24 and 48 h. The weight percent swelling ratio was determined by using the following equation: wt % swelling = 100% * (W_{wet} – W_{dry}) / W_{dry}. By accurately measuring the length (L), width (W), and thickness (D) changes of each sample before and after water immersion, the volume percent swelling ratio was confirmed by the equation: Vol% swelling = 100% * (L_{wet}W_{wet}D_{wet} – L_{dry}W_{dry}D_{dry}) / L_{dry}W_{dry}D_{dry}, where the subscripts dry and wet correspond to the samples before and after water immersion, respectively.

X-ray Photoelectron Spectroscopy. XPS analysis was performed using a Kratos Axis Ultra equipped with a monochromated Al Kr X-ray source. Photoelectrons at pass energies ranging from 20 to 80 eV were collected with a concentric hemispherical analyzer and detected with a delay line detector.

Static Contact Angle and Surface Energy Measurement. Static contact angles were measured using a KSV Instruments LCD CAM 200 optical contact angle meter at room temperature. All measurements were carried out with drops that had a total volume of 10 μL on the surface of each cured film coating on glass using a 1000 μL screw-top syringe. The polar (γ_s^p) and dispersive (γ_s^d) components of the surface free energy of the PFPE/PEG coatings on the substrates were determined according to the Owens–Wendt–Kaelble (OWK) method:^{48,49}

$$\gamma_L = 2 \frac{(\gamma_S^d \gamma_L^d)^{1/2} + (\gamma_S^p \gamma_L^p)^{1/2}}{1 + \cos \theta}$$

where θ is the static contact angle; γ_L is the surface tension of the probe liquid; γ_L^d and γ_L^p are the dispersive component and the polar component of the liquid surface tension, respectively. By measuring the contact angles of two different probe liquids (one polar and one nonpolar) on each surface, the overall solid surface tension can be calculated based on the OWK equation.

Coating Conditioning Prior to *Ulva* Spore Settlement and Growth. Coatings were leached in deionized water for 24 h prior to testing. Following leaching, the coatings were immersed in seawater for 1 h before the start of the experiment.⁴⁰

Settlement of Spores. Zoospores were obtained from mature *Ulva* plants as described previously.⁵⁰ In brief, zoospores were allowed to settle (attach) to test surfaces placed in individual compartments of quadruperm dishes (Greiner) to which 10 mL of zoospore suspension ($1.0 \times 10^6 \text{ mL}^{-1}$) were added. After incubation in the dark at $\sim 20^\circ\text{C}$ for 1 h, the slides were gently washed in seawater to remove unattached zoospores.

Attachment Strength of Sporelings. Samples with attached spores were grown in enriched seawater medium for 7 days to the stage of sporelings (young plants).⁵¹ Sporeling biomass was determined *in situ* by measuring the fluorescence of the chlorophyll contained within the cells with a Tecan fluorescence plate reader. The biomass was quantified in terms of relative fluorescence units (RFU). The RFU value for each slide is the mean of 70 point fluorescence readings.⁵¹

The strength of attachment of sporelings was assessed using a water jet apparatus with individual slides of each treatment being exposed to increasing water pressures.⁵¹ Biomass remaining within the area exposed to the water jet was assessed using the fluorescence plate reader. The percentage removed was calculated from readings taken before and after water jetting. Percentage removal was plotted versus impact pressure and from these curves, the critical impact pressure to remove 50% of the biomass was determined.

Settlement and Removal of Barnacles. To determine the toxicity of the coatings to brine shrimp, all of the coatings were soaked for 6 days in 100 mL of seawater and at 72 h intervals the leachate was removed and replaced with 100 mL of fresh seawater. Samples of the leachate from the coatings were used to conduct assays of survivorship with approximately 100 nauplii larvae of *Artemia* sp. (brine shrimp). The larvae were exposed to the coating leachate and their survival was monitored after 2 days. The survival of the larvae in each coating leachate was compared to leachate from a glass slide control.

Settlement Assay of Barnacle Cypris Larvae. *Balanus amphitrite* cypris larvae were obtained from the Duke University Marine Laboratory. A 400 μL drop of seawater containing 20 to 40, 2–4-day old barnacle cypris larvae was placed on the surface of each coating replicate in a covered Petri dish. The larvae were then placed in an incubator at 25°C with a 12 h light/dark cycle and allowed to settle for 48 h. At the end of the initial assay period the numbers of individuals that successfully attached and metamorphosed were counted. Larvae that did not settle by the end of the 24 h period were observed for signs of abnormal behavior to assess any compromises to normal physiological function. Settlement on each coating formulation was compared to settlement on the glass and T2 controls.^{52,53}

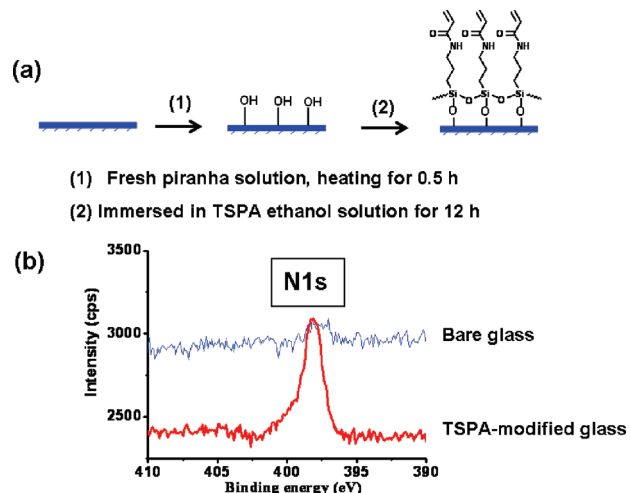


Figure 2. (a) Illustration of the attachment of TSPA onto glass substrate. (b) XPS analysis of unmodified and TSPA-modified glass substrates demonstrating the successful functionalization of the surface.

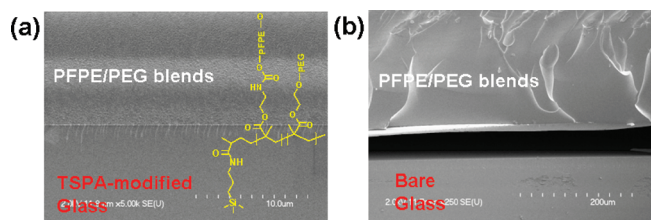
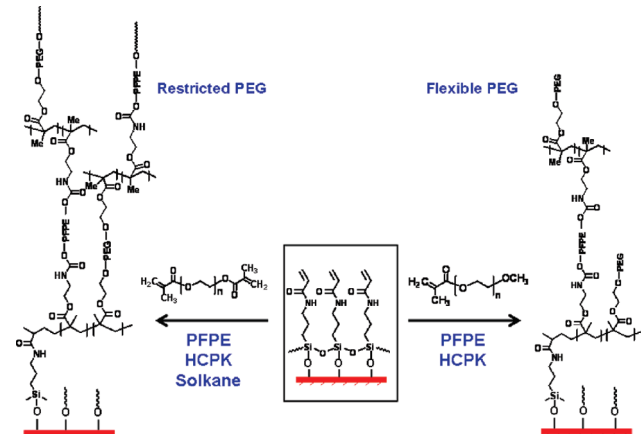


Figure 3. Cured 95:5 PFPE/PEG454-MA coatings on (a) TSPA-modified glass and (b) bare glass.

Scheme 1. Schematic Illustration for the Preparation of Cured PFPE/PEG Coatings on Substrates



Removal Assay of Barnacles. Post settlement, newly metamorphosed juveniles were transferred to growth chambers and kept in an incubator at 25°C with a 12 h light/dark cycle where they were fed a mixture of the unicellular alga *Dunaliella tertiolecta* and the diatom *Skeletonema costatum* for 2 weeks, and then a mixture of *D. tertiolecta*, *S. costatum*, and naupliar larvae of *Artemia* sp. for an additional week. Barnacles were then transferred to a 16-L aquaria tank in an automated rack system with temperature, salinity and pH monitors and a programmed 10% daily water change. Barnacles in the tank were fed a 500-mL flask of *Artemia* sp. three times per week for another 4–6 weeks, which is the time it took the juvenile barnacles to reach a basal plate diameter of 3–5 mm, the minimum size necessary to conduct force gauge tests. Prior to

Table 1. Water-Uptake and Percent Swelling of PFPE/PEG454–MA Cross-Linked Networks of Different Weight Ratios^a

		blends (weight ratio)						
		PFPE	PFPE/ PEG454– MA (95:5)	PFPE/ PEG454– MA (90:10)	PFPE/ PEG454– MA (85:15)	PFPE/ PEG454– MA (80:20)	PFPE/ PEG454– MA (70:30)	PFPE/ PEG454– MA (50:50)
in H ₂ O 24 h	weight increase (%)	0.09	0.22	0.56	2.34	8.02	21.79	67.34
	volume swelling (%)	1.68	3.16	4.07	22.15	29.10	46.64	86.12
in H ₂ O 48 h	weight increase (%)	0.12	0.28	0.72	3.32	9.36	21.82	66.41
	volume swelling (%)	2.62	3.91	5.77	18.47	31.97	44.20	86.34

^aCross-linked networks indicated in italics had the lowest percent swelling and water-uptake values and therefore were the focus of further study.

Table 2. Water-Uptake and Percent Swelling in Water of PFPE/PEG550–DMA Cross-Linked Networks with Different Weight Ratios^a

		blends (weight ratio)				
		PFPE/PEG ₅₅₀ – DMA (95:5)	PFPE/PEG ₅₅₀ – DMA (90:10)	PFPE/PEG ₅₅₀ – DMA (70:30)	PFPE/PEG ₅₅₀ – DMA (50:50)	PFPE/PEG ₅₅₀ – DMA (30:70)
in H ₂ O 24 h	weight change (%)	0.28	0.45	2.13	4.69	8.49
	volume change (%)	0.36	1.08	2.45	10.89	19.24
in H ₂ O 48 h	weight change (%)	0.26	0.49	2.44	3.74	6.92
	volume change (%)	0.33	2.31	2.31	10.86	18.04

^aCross-linked networks indicated in italics had the lowest percent swelling and water-uptake values and therefore were the focus of further study.

Before water immersion



After water immersion for 24 h



Figure 4. Stability of the cured PFPE/PEG coatings on TSPA treated glass substrates against water immersion.

removal, a digital photograph was taken of each barnacle basal plate using a Canon EOS 10D camera attached to an Olympus SZX12 dissecting microscope. Each slide was then clamped into the force-gauge apparatus, which consisted of an IMADA ZP-11 digital force gauge mounted on an IMADA SV-5 motorized test stand and a custom chamber that houses the slide immersed in seawater; thus allowing the testing of the force necessary to remove the barnacles in shear and in situ. The barnacles were removed with the force gauge with the force applied in shear at a rate of 4.5 N s⁻¹ and the maximum force was recorded. If barnacles removed wholly from the coating, the critical removal stress, CRS, (N/mm²) was calculated by dividing the force

measured by the area of the basal plate. The photographs of the basal plates were used to determine their area using NIH's ImageJ. The average CRS for each coating was compared against the control groups. If the barnacle broke and its basal plate was partially removed, the remaining basal plate was photographed again and the exact percentage remaining after removal testing was calculated.

Results and Discussion

Using UV-initiated free radical polymerization techniques, dimethacryloxy-functionalized PFPE–DMA materials were cross-linked into networks with monomethacryloxy-functionalized PEG454–MA or dimethacryloxy-functionalized PEG550–DMA in the presence of a photoinitiator. Interestingly, it was found that PFPE–DMA is miscible with PEG454–MA forming completely clear miscible liquid solutions. However, PEG550–DMA did not form a miscible solution with PFPE–DMA. The resulting milky mixture was observed to quickly macro-phase separate after vortexing. However it was found that by incorporating 10% (v/w) of the cosolvent Solkane both the PFPE–DMA and PEG550–DMA formed a miscible solution. Upon addition of 0.2% HCPK photoinitiator and exposure to UV-irradiation for 10 min under N₂ purge these solutions were observed to cure as fully cross-linked elastomers. Typically, by casting the photocurable blends in a 1 mm × 35 mm × 75 mm PDMS mold, a series of size specific PFPE/PEG films were obtained.

The PFPE/PEG blends were cured on glass substrates. However delamination from the substrate was found to be a frequent problem for these low surface energy PFPE blends. Therefore, in order to minimize delamination between the cured film and the glass slide, a layer of *N*-(trimethoxysilyl)propylacrylamide, TSPA, was deposited on the substrate surface via the hydrolysis of the trimethoxysilyl groups by the hydroxyl groups on the glass surface. The methacrylamide moiety was then able to be covalently incorporated with PFPE/PEG blends when exposed to UV-irradiation minimizing the delamination issues. Successful modification of the glass substrate was verified by XPS analysis as indicated by the appearance of the N1s peak at 398 eV (Figure 2). Casting and photocuring a film of a PFPE/PEG blend onto the TSPA

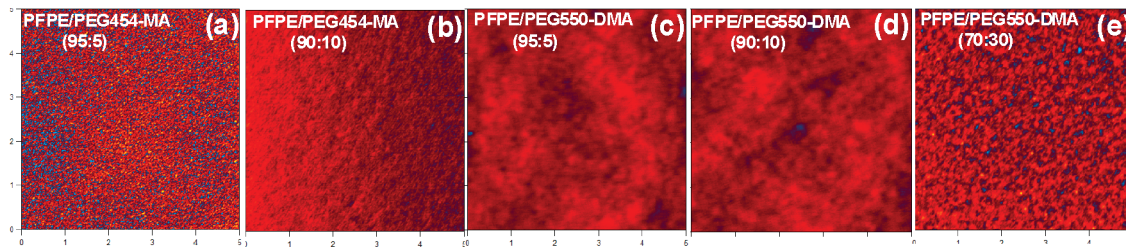


Figure 5. Surface topographies of the cured PFPE/PEG coatings on the substrates by AFM observation (a–e). Height images are $5 \times 5 \mu\text{m}$.

Table 3. Summarized Characterizations of PFPE/PEG Cross-Linked Networks Including Static Contact Angle by Using Water and Hexadecane, Surface Energy, Young's Modulus, Surface Roughness, and Transparency

	coatings					
	PFPE	PFPE/PEG454-MA (95:5)	PFPE/PEG454-MA (90:10)	PFPE/PEG550-DMA (95:5)	PFPE/PEG550-DMA (90:10)	PFPE/PEG550-DMA (70:30)
contact angle (water)	109.5 ± 2.0	111.3 ± 0.6	112.3 ± 2.4	106.3 ± 2.1	108.4 ± 2.3	109.6 ± 1.1
contact angle (hexadecane)	67.7 ± 0.7	67.9 ± 1.4	69.3 ± 0.6	69.5 ± 1.7	68.7 ± 1.5	68.9 ± 1.4
surface energy (mN/m)	14.2	13.9	13.3	14.4	14.1	13.9
modulus (MPa)	13.20 ± 0.66	8.89 ± 0.50	6.13 ± 0.57	12.57 ± 1.71	11.86 ± 1.39	8.47 ± 0.53
surface roughness (nm)	0.89	1.25	1.36	1.19	1.35	2.27
transparency (%)	97.2	96.1	94.9	95.9	94.7	91.4

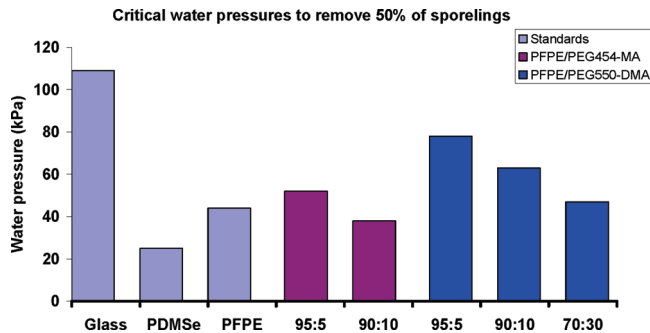


Figure 6. Critical water surface pressures for 50% removal of sporelings from PFPE/PEG coatings. The points are derived from detachment curves and read off the lines as 50% values, consequently an error bar cannot be put on the data. The data show the relative ranking of each sample in terms of fouling-release.

modified substrate resulted in a robust coating that was firmly attached to the substrate (Scheme 1). After curing, the residual Solkane in the PFPE/PEG-DMA coatings was removed under vacuum at room temperature overnight. Taking the 95:5 PFPE/PEG454-MA as an example, the cross section of Figure 3a shows that the film has been tightly bound to the TSPA-modified glass substrate. Conversely, as shown in Figure 3b, clear delamination was observed when the film was coated on bare glass, demonstrating the benefit of using TSPA-functionalized glass to enhance the attachment of the PFPE/PEG blend films to the substrate.

Low water-uptake and high stability of coatings on substrates are needed for marine applications. Since PEG is hydrophilic, as the PEG content in the PFPE/PEG coatings is increased the coatings will increasingly swell and offer poor water resistance when the PEG content is above some critical amount. To address this issue, the water uptake and the swelling degree of each cured PFPE/PEG coating were determined. As shown in Table 1, the water uptake and volume swelling degree of PFPE/PEG454-MA gradually increase as more PEG454-MA was incorporated into the blends. When the PEG454-MA content reached 15 wt %, the films were found to swell greatly with an increase of 22.15% in volume after 24 h of immersion in water.

When 10 wt % or less of the PEG454-MA was incorporated into the blends, the films displayed high water-resistance with a low degree of swelling. In similar fashion, the PFPE/PEG550-DMA blends were seen to remain relatively unchanged when the PEG550-DMA content was not more than 30 wt % in the blends, as shown in Table 2. Cured films with 30 wt % or less PEG content were found to maintain integrity on the substrates after 24 h water immersion, as shown in Figure 4. However, for example, the coating with 50 wt % PEG550-DMA content was observed to fracture and peel off the substrate due to a large, swelling-induced stress. Typically, the stable PFPE/PEG coating films, including PFPE/PEG454-MA (95:5, 90:10) and PFPE/PEG550-DMA (95:5, 90:10, 70:30), were selected as candidates for the subsequent fouling-release studies.

The surface topographies of the cured PFPE/PEG blends were investigated by AFM. As shown in Figure 5a–e, AFM results indicate that the gradual addition of PEG has a slight affect on the cured surface structure, suggesting phase separation existing between the PFPE and PEG. This increase in surface roughness and the existence of microphase separation is particularly clear in the 70:30 PFPE/PEG550-DMA sample, as seen in Figure 5e. AFM measurement of the surface roughness of the various cured PFPE/PEG blends compared to a cured neat PFPE-DMA sample reveal an increase in roughness with increasing PEG content (Table 3). The neat PFPE sample has a surface roughness of less than 1 nm while the 70:30 PFPE/PEG550-DMA sample has a roughness of 2.27 nm. Interestingly, the roughness appears to be irrespective of the PEG functionality as the 95:5 PFPE/PEG-MA and PFPE/PEG-DMA samples have roughly the same roughness (1.25 and 1.19 nm, respectively) as do the 90:10 PFPE/PEG-MA and PFPE/PEG-DMA samples (1.36 and 1.35 nm, respectively). The AFM observations are in agreement with the optical transparency results. As shown in Table 3, the optical transparency of the resulting films was quantitatively elucidated by measuring the transmittance at 550 nm. The cured films of the PFPE/PEG blends showed high transmittance, but a slight decrease is observed upon the increased addition of PEG, indicative of immiscibility between the PFPE and PEG components in these blends resulting in microscale phase separation.⁴⁶

The product of the surface energy of a given material and its Young's modulus has been reported to be a good predictor of the

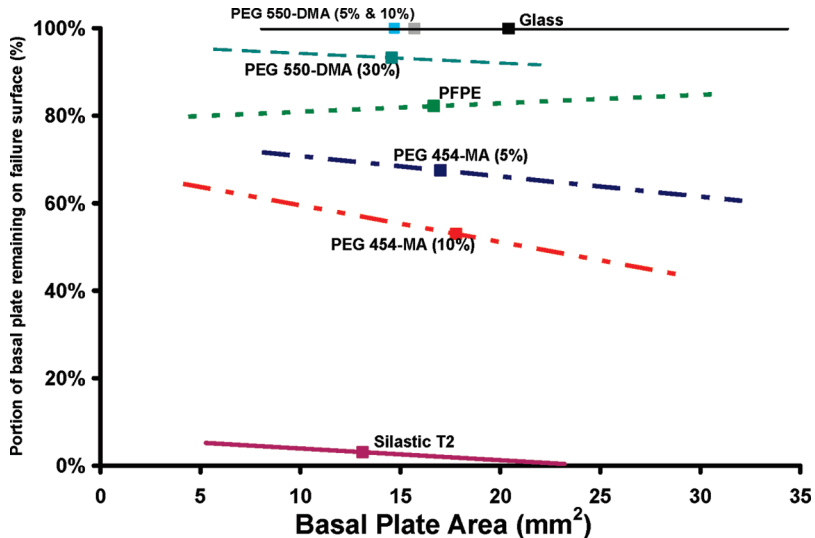


Figure 7. Percentage of basal plate remaining as a function of the basal plate area prior to removal. Coatings that exhibited 100% remaining basal plate lie on the same line as the glass control. Silastic T2 is shown as a representative foul-release surface; data for T2 were collected during a different experiment.

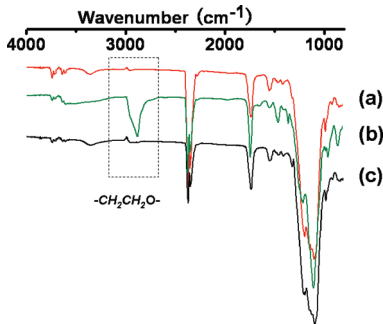


Figure 8. ATR-FTIR spectra: (a) PFPE coating; (b) 90:10 PFPE/PEG454-MA coating; (c) 90:10 PFPE/PEG550-DMA coating.

coating fouling release performance against certain organisms.^{13,14} The surface energy of each cured PFPE/PEG blend was evaluated using static contact angles by the Owens–Wendt–Kaelble (OWK) method and Young's modulus was calculated from the slope of the stress–strain curve obtained using an Instron. In the OWK method, by measuring two static contact angles of two liquids, including one polar solvent (e.g. water) and one apolar solvent (e.g., hexadecane) whose γ^d and γ^p values are known, the surface free energy can be calculated. Since the relative content of PEG was kept low in the blends, all the cured films exhibited low surface energies ranging from 13.3 to 14.4 mN/m as a result of the high content of low surface energy PFPE in the matrix. The modulus of the films was observed to significantly decrease as the PEG454-MA content was increased because the degree of cross-linking was reduced by incorporation of the monofunctional PEG454-MA. As shown in Table 3, compared to the Young's modulus of pure PFPE–DMA of 13.20 MPa, the addition of 10 wt % PEG454-MA to the blend was seen to decrease the Young's modulus to 6.13 MPa. The incorporation of PEG550–DMA into the PFPE/PEG blends was also seen to decrease the Young's modulus of the PFPE–DMA, but not as dramatically as seen when incorporating PEG–MA due to the difunctionality of the PEG–DMA macromonomer.⁴⁶ For instance, when 10 wt % of PEG550–DMA was incorporated into the network the blend had a Young's modulus of 11.86 MPa, in comparison the 90:10 PFPE/PEG454-MA blend has a modulus of 6.13 MPa. The product of surface energy and Young's modulus of the cured PFPE/PEG blends can be tuned

through the selection of either mono- or difunctional PEG and varying its weight ratio in the blend with PFPE–DMA. Since the modulus and surface energy values for 95:5 PFPE/PEG454–MA and 70:30 PFPE/PEG550–DMA are similar, the product values are also approximately same and therefore these materials are expected to exhibit similar fouling release performance.

The fouling release performance of the PFPE/PEG coatings was evaluated by studying the release of sporelings (young plants) the green fouling seaweed *Ulva*. After 7 days of growth, a green lawn of sporelings covered all of the test surfaces, the amounts of biomass on all the PFPE/PEG coatings being similar (data not shown). Since the sporelings grew normally on all of the PFPE/PEG coatings with no signs of toxicity, these coating films could be considered as environmentally benign coatings. To determine the strength of attachment of sporelings to each type of PFPE/PEG coating, ease of removal was assessed using a water jet apparatus with individual slides of each treatment being exposed to increasing water jet pressures. The critical water pressures (Figure 6) to remove 50% of the biofilms were calculated from plots of percentage removal versus water impact pressure. In the PFPE/PEG454–MA blends the strength of attachment of the sporelings decreased as the PEG454–MA content increased from 5 to 10%, i.e., a lower critical impact pressure was needed to removed 50% of the biomass. Similarly, the strength of attachment of the sporelings to the PFPE/PEG550–DMA blends also decreased as the PEG content of the coating increased from 5–30 wt %. At the highest loading of 30 wt % PEG550–DMA, the sporelings had a similar attachment strength to that of the pure PFPE and the 95:5 PFPE/PEG454–MA coating. The best fouling-release performance was observed for the 90:10 PFPE/PEG454–MA coating.

Additionally, the PFPE/PEG454–MA coatings were also found to display better barnacle removal performance than the PFPE/PEG550–DMA coatings. In fact, of the experimental coatings tested, PFPE/PEG454-MA (90:10) showed the best fouling-release performance, although not as good as PDMS standards. It should be noted that none of the leachate samples from the coatings were found to be toxic to brine shrimp, supporting the possibility that PFPE/PEG blends can be employed as environmentally benign materials for fouling release. Upon removal, most of the barnacles that were removed from the test coatings broke leaving part or all of the basal plate attached to the coating surface. When breakage occurs, the force measured is the

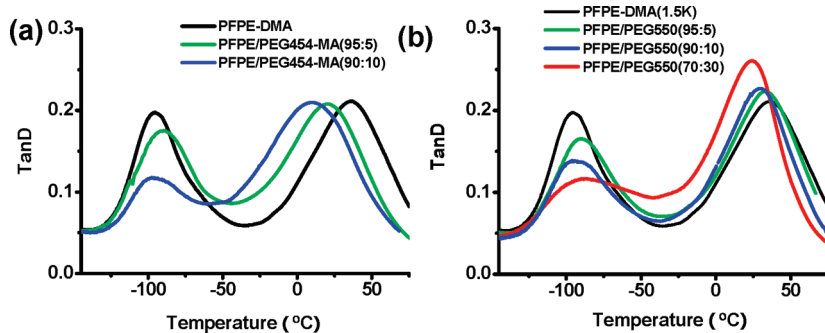


Figure 9. DMTA spectra: (a) cured PFPE/PEG454-MA blends of different weight ratios; (b) cured PFPE/PEG550-DMA blends of different weight ratios.

cohesive force of the barnacle to itself and not the force of adhesion of the barnacle to the surface; therefore critical removal stress (CRS) can not be calculated. Berglin et al. suggest that the remaining fraction of the basal plate left on a surface appears to be a function of barnacle bioadhesive bond strength and that it could be used as a measure of the efficacy of foul-release coatings.⁵² As shown in Figure 7, coatings of PFPE/PEG454-MA perform relatively well compared to our other experimental coatings. For example, PFPE/PEG454-MA have a lower average percentage of basal plate remaining than do PFPE and PFPE/PEG550-DMA, which often left behind the entire basal plate on attempted removal; a result similar to glass controls, to which barnacles readily attached with great tenacity. In addition to having a lower basal plate percentage remaining compared to our other coatings, PFPE/PEG454-MA have a steeper negative slope, which further supports better fouling release performance, because the shift in mode of failure upon removal occurs at smaller sizes. For comparison, the fouling-release control surface, Silastic T2, had a very low percentage of basal plate remaining and the slope of line is much steeper than our experimental coatings (Figure 7). The average CRS for animals on Silastic T2 is 0.149 N/mm².

The product of surface energy and Young's modulus has been found to not be an accurate predictor for the fouling release performance of these amphiphilic PFPE/PEG coatings, since the product of surface energy and Young's modulus of the PFPE/PEG454-MA (95:5) and PFPE/PEG550-DMA (70:30) materials are approximately same but the 95:5 PFPE/PEG454-MA coating had much better barnacle release performance. It is anticipated that the free PEG chains are flexible in the PFPE/PEG454-MA blends which can migrate out to the surface in a hydrophilic environment and therefore provide enhanced biofouling performance. But the more densely cross-linked PEG chains in the PFPE/PEG550-DMA blends are restricted due to the difunctionality of the oligomers and therefore are not able to migrate to the surface as easily. In light of this hypothesis, it can be understood why the PFPE/PEG454-MA blends perform much better in comparison to the PFPE/PEG550-DMA coatings as the flexible PEG454-MA is more likely to migrate to the surface to weaken fouling attachment. In addition to surface chemistry segregation, the product of the surface energy and Young's modulus also does not account for differences in surface roughness. This is believed to be the reason why the 70:30 PFPE/PEG550-DMA sample, though possessing the highest PEG content also has the roughest surface of all the materials tested, and hence does not perform any better in biofouling testing than the smooth PFPE-DMA sample.

The presence of PEG on the PFPE/PEG454-MA surface was confirmed by ATR-FTIR as shown in Figure 8. The absorbance at 2980 cm⁻¹ is ascribed to the stretching vibration of $-\text{CH}_2-$ of the PEG segments. Typically, the IR intensity at 2980 cm⁻¹ of

90:10 PFPE/PEG454-MA is much stronger than that of 90:10 PFPE/PEG550-DMA blend. The higher intensity of PFPE/PEG454-MA of Figure 8b indicates the existence of flexible PEG chains on this coating surface. On the other hand, the more restricted PEG chains of the PFPE/PEG550-DMA coating has a weaker IR intensity at 2980 cm⁻¹ indicating that there is less PEG on the surface, as shown in Figure 8c.

The feature of flexible PEG segment in the PFPE/PEG454-MA blend was additionally interrogated by DMTA of the bulk materials. Two transitions were found for the cured PFPE-DMA, the glass transition (T_g) at 37.2 °C was assigned to the cross-linked methacrylate end group domains and a secondary relaxation peak at -95.4 °C was assigned to the PFPE fluorocarbon domains of the main chains located away from cross-links. As shown in Figure 9a, for the blends of PFPE-DMA with PEG454-MA, the methacrylate groups of the PFPE segments are miscible with the methacrylate groups of PEG segments and formed a polymethacrylate domain after cross-linking, corresponding to the broad T_g from 0 to 35 °C, which gradually shifts to a lower temperature with increasing PEG in the composition ratio. The decrease in T_g upon addition of PEG454-MA indicates that the side chain of PEG moves freely which should be induced by the flexible PEG grafting branches. However, for the blends of PFPE with PEG550-DMA (Figure 9b), in which the side PEG chains of polymethacrylate are well cross-linked in the networks which actually did not enhance the freedom of main chain of polymethacrylate, the T_g nearly maintained unchanged upon gradual addition of PEG550-DMA.

Conclusion

Herein we have presented a facile approach for the preparation of amphiphilic hydrophilic/fluorophilic cross-linked networks via photocuring for fouling-release coating applications. A range of networks composed of elastomeric perfluoropolyether (PFPE) and poly(ethylene glycol), in which the PFPE was cross-linked with PEG through the copolymerization of methacryloxy-functionalized end groups. These coatings maintained a low surface energy and displayed low swelling characteristics as a function of water when less than 10% PEG454-MA or 30% PEG550-DMA is blended, promising high stability for potential application. In particular, the PFPE/PEG454-MA (10%) coating displayed better fouling-release performance when evaluated against *Ulva* and removal of juvenile barnacles in comparison to all the PFPE/PEG550-DMA coatings, which is attributed to the flexibility of PEG454-MA chains allowing the PEG to migrate to the surface of the PFPE/PEG454-MA blend. Without complicated synthesis, the functionalized PFPE blends with monomethacryloxy-functionalized PEG were found to be well suited as photocurable coatings on the substrates. Since the PFPE/PEG coatings are nontoxic and the liquid precursors are easily applied it is hoped that this new family of photocurable

amphiphilic blends can be applied as minimally adhesive, mechanically durable, nonfouling/fouling-release coatings in marine applications. Although the fouling-release attributes of these coatings are not as good as the PDMSe standard, this research is providing an understanding on how to tune fouling-release properties based on PEG flexibility. Highly efficient fouling-release coatings are being pursued by tuning bulk stiffness, PEG length, surface segregation, and surface roughness.

Acknowledgment. This work was supported by the Office of Naval Research under Grant No. N00014-02-1-0185 as well as the STC program of the National Science Foundation for shared facilities. J.A.C. and M.E.C. also acknowledge support from ONR under Grant No. N00014-08-1-0010. Dr. Zhaokang Hu, Dr. Meredith Hampton, and Dr. Stuart Williams of UNC-CH are acknowledged for their helpful discussion on PFPE materials. Dr. Carrie Donley of UNC-CH performed the XPS experiments at the Chapel Hill Analytical & Nanofabrication Laboratory (CHANL).

References and Notes

- (1) Finnie, A. A.; Williams, D. N., *Paint and Coatings Technology for the control of Marine Fouling*. In *Biofouling*; Durr, S., Thomason, J. C., Eds.; Wiley-Blackwell: New York, 2010, pp 185–206.
- (2) Thomas, K. V.; Brooks, S. *Biofouling* **2010**, *26*, 73.
- (3) Omae, I. *Appl. Organomet. Chem.* **2003**, *17*, 81.
- (4) Anderson, C.; Atlar, M.; Callow, M. E.; Candries, M.; Milne, A.; Townsin, R. L. *J. Marine Des. Oper.* **2003**, *4*, 11.
- (5) Callow, M. E.; Callow, J. A.; Clare, A. S. *Some new insights into marine biofouling*. *World Super Yacht* **2003**, Issue 1, pp 34–39.
- (6) Schumacher, J. F.; Aldred, N.; Callow, M. E.; Finlay, J. A.; Callow, J. A.; Clare, A. S.; Brennan, A. B. *Biofouling* **2007**, *23*, 307.
- (7) Efimenko, K.; Finlay, J.; Callow, M. E.; Callow, J. A.; Genzer, J. *ACS Appl. Mater. Interfaces* **2009**, *1*, 1031.
- (8) Genzer, J.; Efimenko, K. *Biofouling* **2006**, *22*, 339.
- (9) Webster, D. C.; Chisholm, B. J.; Stafslie, S. J. *Biofouling* **2007**, *23*, 179.
- (10) Ekin, A.; Webster, D. C.; Daniels, J. W.; Stafslie, S. J.; Casse, F.; Callow, J. A.; Callow, M. E. *J. Coatings Tech. Res.* **2007**, *4*, 435.
- (11) Grozea, C. M.; Gunari, N.; Finlay, J. A.; Grozea, D.; Callow, M. E.; Callow, J. A.; Lu, Z.-H.; Walker, G. C. *Biomacromolecules* **2009**, *10*, 1004.
- (12) Zhang, Z.; Finlay, J. A.; Wang, L.; Gao, Y.; Callow, J. A.; Callow, M. E.; Jiang, S. *Langmuir* **2009**, *25*, 13516.
- (13) Brady, R. F.; Singer, I. L. *Biofouling* **2000**, *15*, 73.
- (14) Berglin, M.; Lönn, N.; Gatenholm, P. *Biofouling* **2003**, *195*, 63.
- (15) Baier, R. E.; Meyer, A. E. *Biofouling* **1992**, *6*, 165.
- (16) Swain, G. W. *Prot. Coat. Eur.* **1999**, *4*, 18.
- (17) Singer, I. L.; Kohl, J. G.; Patterson, M. *Biofouling* **2000**, *16*, 301.
- (18) Mera, E.; Wynne, K. J. *US Patent* 6,265,515 B1, July 24, 2001.
- (19) Grunlan, M. A.; Lee, N. S.; Cai, G.; Gäddä, T.; Mabry, J. M.; Mansfeld, F.; Kus, E.; Wendt, D. E.; Kowalke, G. L.; Finlay, J. A.; Callow, J. A.; Callow, M. E.; Weber, W. P. *Chem. Mater.* **2004**, *16*, 2433.
- (20) Gu, L.; Santra, S.; Mericle, R. A.; Kumar, A. V. *J. Biomech.* **2005**, *38*, 1221.
- (21) Stein, J.; Truby, K.; Wood, D. C.; Takemori, M.; Vallance, M.; Swain, G.; Kavanagh, C.; Kovach, B.; Schultz, M.; Wiebe, D.; Holm, E.; Montemarano, J.; Wendt, D.; Smith, C.; Meyer, A. *Biofouling* **2003**, *19*, 87.
- (22) Yarbrough, J. C.; Rolland, J. P.; DeSimone, J. M.; Callow, M. E.; Finlay, J. A.; Callow, J. A. *Macromolecules* **2006**, *39*, 2521.
- (23) Nakamura, I.; Yamamori, N. U.S. Patent 5914357, 1999; *Chem. Abstr.* **1997**, *126*, 279096.
- (24) Nakamura, I. Japan Patent Kokai H11-256077, 1999; *Chem. Abstr.* **1999**, *131*, 230092.
- (25) Majumdar, P.; Lee, E.; Patel, N.; Ward, K.; Stafslie, S. J.; Daniels, J.; Chisholm, B. J.; Boudjouk, P.; Callow, M. E.; Callow, J. A.; Thompson, S. E. M. *Biofouling* **2008**, *24*, 185.
- (26) Truby, K.; Wood, C.; Stein, J.; Cell, J.; Carpenter, J.; Kavanagh, C.; Swain, G.; Wiebe, D.; Lapota, D.; Meyer, A.; Holm, E.; Wendt, D.; Smith, C.; Montemarano, J. *Biofouling* **2000**, *15*, 141.
- (27) Marabotti, I.; Morelli, A.; Orsini, L. M.; Martinelli, E.; Galli, G.; Chiellini, E.; Lien, E. M.; Pettitt, M. E.; Callow, M. E.; Callow, J. A.; Conlan, S. L.; Mutton, R. J.; Clare, A. S.; Kocjan, A.; Donik, C.; Jenko, M. *Biofouling* **2009**, *25*, 481.
- (28) Omae, I. *Chem. Rev.* **2003**, *103*, 3431.
- (29) Langer, R. *Nature* **1998**, *392*, 5.
- (30) Chapman, R. G.; Ostuni, E.; Takayama, S.; Holmlin, R. E.; Yan, L.; Whitesides, G. M. *J. Am. Chem. Soc.* **2000**, *122*, 8303.
- (31) Ostuni, E.; Chapman, R. G.; Holmlin, R. E.; Takayama, S.; Whitesides, G. M. *Langmuir* **2001**, *17*, 5605.
- (32) Herrwerth, S.; Eck, W.; Reinhardt, S.; Grunze, M. *J. Am. Chem. Soc.* **2003**, *125*, 9359.
- (33) Jeon, S. I.; Lee, J. H.; Andrade, J. D.; DeGennes, P. G. *J. Colloid Interface Sci.* **1991**, *142*, 149.
- (34) Zheng, J.; Li, L.; Chen, S.; Jiang, S. *Langmuir* **2004**, *20*, 8931.
- (35) Harder, P.; Grunze, M.; Dahint, R.; Whitesides, G. M.; Laibinis, P. E. *J. Phys. Chem. B* **1998**, *102*, 426.
- (36) Ekblad, T.; Bergström, G.; Ederth, T.; Conlan, S. L.; Mutton, R.; Clare, A. S.; Wang, S.; Liu, Y.; Zhao, Q.; D'Souza, F.; Donnelly, G. T.; Willemsen, P. R.; Pettitt, M. E.; Callow, M. E.; Callow, J. A.; Liedberg, B. *Biomacromolecules* **2008**, *9*, 2775.
- (37) Gan, D.; Mueller, A.; Wooley, K. L. *J. Polym. Sci., Part A: Polym. Chem.* **2003**, *41*, 3531.
- (38) Gudipati, C. S.; Greenlief, C. M.; Johnson, J. A.; Prayongpan, P.; Wooley, K. L. *J. Polym. Sci., Part A: Polym. Chem.* **2004**, *42*, 6193.
- (39) Gudipati, C. S.; Finlay, J. A.; Callow, J. A.; Callow, M. E.; Wooley, K. L. *Langmuir* **2005**, *21*, 3044.
- (40) Krishnan, S.; Ayothi, R.; Hexmer, A.; Finlay, J. A.; Sohn, K. E.; Perry, R.; Ober, C. K.; Kramer, E. J.; Callow, M. E.; Callow, J. A.; Fisher, D. A. *Langmuir* **2006**, *22*, 5075.
- (41) Krishnan, S.; Wang, N.; Ober, C. K.; Finlay, J. A.; Callow, M. E.; Callow, J. A.; Hexemer, A.; Sohn, K. E.; Kramer, E. J.; Fischer, D. A. *Biomacromolecules* **2006**, *7*, 1449.
- (42) Weinman, C. J.; Finlay, J. A.; Park, D.; Paik, M. Y.; Krishnan, S.; Sundaram, H. S.; Dimitriou, M.; Sohn, K. E.; Callow, M. E.; Callow, J. A.; Handlin, D. L.; Willis, C. L.; Kramer, E. J.; Ober, C. K. *Langmuir* **2009**, *25*, 12266.
- (43) Martinelli, E.; Agostini, S.; Galli, G.; Chiellini, E.; Glisenti, A.; Pettitt, M. E.; Callow, M. E.; Callow, J. A.; Graf, K.; Bartels, F. W. *Langmuir* **2008**, *24*, 13138.
- (44) Maynor, B. W.; LaRue, I.; Hu, Z.; Rolland, J. P.; Pandya, A.; Fu, Q.; Liu, J.; Spontak, R. J.; Sheiko, S. S.; Samulski, R. J.; Samulski, E. T.; DeSimone, J. M. *Small* **2007**, *3*, 845–849.
- (45) Hu, Z.; Finlay, J. A.; Chen, L.; Betts, D. E.; Hillmyer, M. A.; Callow, M. E.; Callow, J. A.; DeSimone, J. M. *Macromolecules* **2009**, *42*, 6999.
- (46) Hu, Z. K.; Chen, L.; Betts, D. E.; Pandya, A.; Hillmyer, M. A.; DeSimone, J. M. *J. Am. Chem. Soc.* **2008**, *130*, 14244.
- (47) Rolland, J. P.; Van Dam, R. M.; Schorzman, D. A.; Quake, S. R.; DeSimone, J. M. *J. Am. Chem. Soc.* **2004**, *126*, 2322.
- (48) Owens, D. K.; Wendt, R. C. *J. Appl. Polym. Sci.* **1969**, *13*, 1741.
- (49) Kaelble, D. H. *J. Adhes.* **1970**, *2*, 66.
- (50) Callow, M. E.; Callow, J. A.; Pickett-Heaps, J. D.; Wetherbee, R. *J. Phycol.* **1997**, *33*, 938.
- (51) Finlay, J. A.; Fletcher, B. R.; Callow, M. E.; Callow, J. A. *Biofouling* **2008**, *24*, 219.
- (52) Berglin, M.; Larsson, A.; Jonsson, P. R.; Gatenholm, P. *J. Adhes. Sci. Technol.* **2001**, *15*, 1485.
- (53) Wendt, D. E.; Kowalke, G. L.; Kim, J.; Singer, I. L. *Biofouling* **2006**, *22*, 1.